Radiation Physics and Chemistry 167 (2020) 108319

Contents lists available at ScienceDirect

Radiation Physics and Chemistry

journal homepage: www.elsevier.com/locate/radphyschem

Determination of the penumbra width of Elekta SRS cone collimator for 6 MV FF and 6 MV FFF energies using gradient-based edge detection

Daniela P. Groppo[a,b,*], Crystian W.C. Saraiva[c], Linda V.E. Caldas[a]

[a] Instituto de Pesquisas Energéticas e Nucleares, Comissão Nacional de Energia Nuclear (IPEN/CNEN), Av. Prof. Lineu Prestes, 2242, São Paulo, Brazil
[b] Hospital das Americas, Centro de Oncologia Integrado, Av. Jorge Cury, 550, Rio de Janeiro, Brazil
[c] Hospital do Coração – HCor, R. Desembargador Eliseu Guilherme, 147, São Paulo, Brazil

ARTICLE INFO

Keywords:
Small field dosimetry
Stereotactic radiotherapy
SRS cone collimator

ABSTRACT

The dosimetric measurements of small fields of radiation are undertaken with detectors such as: GafchromicTM films, diodes, diamond detectors and ionization chambers of small volumes. The penumbra width, e.g. the spatial distance between 80% and 20% dose, is smaller in small fields. This fact increases the curvature and hence the volume effect in the penumbra region. The accuracy in the penumbra calculation is important at the QA test for implementation of the cranial Stereotactic Radiosurgery. The objective of this work was to apply a Gradient-Based Edge Detection plugin to calculate the penumbra of a radiation beam defined with the Elekta SRS Cone Collimators for beams of 6 MV (Flattening Filter – FF) and 6 MV (Flattening Filter Free – FFF) energies using the beam profile obtained with GafchromicTM film. The results corroborate those from the literature, and they allow a quantitative evaluation of the width of dosimetric penumbra by Gradient-Based Edge Detection.

1. Introduction

The concept of stereotactic radiosurgery (SRS) was introduced by the neurosurgeon Lars Leksell in 1951 (Schell et al., 1995). SRS is an irradiation method used to deliver a single and high absorbed dose of radiation in a small intracranial target volume through the intact skull. Therefore, it requires high accuracy and high conformity. One of the major problems with dosimetry used in SRS is the use of small fields (micro-MLC or circular collimator). It is known that small field dosimetry is complex due to the lack of equilibrium of charged particles, partial occlusion of the source and effect of volume versus detector size. Dosimetry technical reports and task groups, such as IAEA TRS-398 (IAEA, 2006) and AAPM TG -51 (AAPM , 1999) provide guidelines for traditional radiation fields (from 3 cm × 3 cm–40 cm × 40 cm).

Circular collimation systems for SRS allow the use of small fields. An evaluation consistent of their mechanical, geometric and dosimetric parameters is necessary for correct and assurance use of these small fields. In this type of collimation systems, the inner surface presents the same behavior of the divergence of the beam, which reduces the penumbra transmission. Although it is possible to reduce the effect of the transmission penumbra with the design of the circular cones, it is not possible the complete removal of this effect. The penumbra concept, in general, consists of a consensus, and it means the region of the field edge, in which the dose rate is reduced as a distance function of the central axis of the beam.

The penumbra transmission corresponds to the region irradiated by photons that are transmitted by the edge of the collimation system. Another type of penumbra, also known as geometric penumbra, mainly defined by the collimation geometry of the radiation source (primary, secondary and tertiary, when applicable), source size and source-surface distance (SSD). It can be determined using the mathematical formalism of triangle similarity.

In this study, the parameter evaluated is the penumbra width of this collimation system for different sizes of cone collimators, ranging from 5 mm to 35 mm in diameter. The penumbra characterization of a circular collimation system depends on: alignment of the collimation system with the central axis of the radiation beam, distance from the collimator to the radiation source, dimensions of the source and distance from the source to the measuring plane.

In order to measure the thickness of the geometric penumbra there are different methodologies, in which the uncertainties also depend on the detector. According to TRS 483 (IAEA, 2017), the most suitable detectors for determining the penumbra in small fields are tissue equivalent radiochromic film, diodes, diamond detectors, small air-filled ionization chambers and liquid chambers. For this reason, the penumbra was evaluated using radiochromic film. A mathematical

* Corresponding author. Instituto de Pesquisas Energéticas e Nucleares, Comissão Nacional de Energia Nuclear (IPEN/CNEN), Av. Prof. Lineu Prestes, 2242, São Paulo, Brazil.

E-mail address: dpgroppo@usp.br (D.P. Groppo).

https://doi.org/10.1016/j.radphyschem.2019.05.009
Received 15 December 2018; Received in revised form 30 April 2019; Accepted 4 May 2019
Available online 06 May 2019
0969-806X/

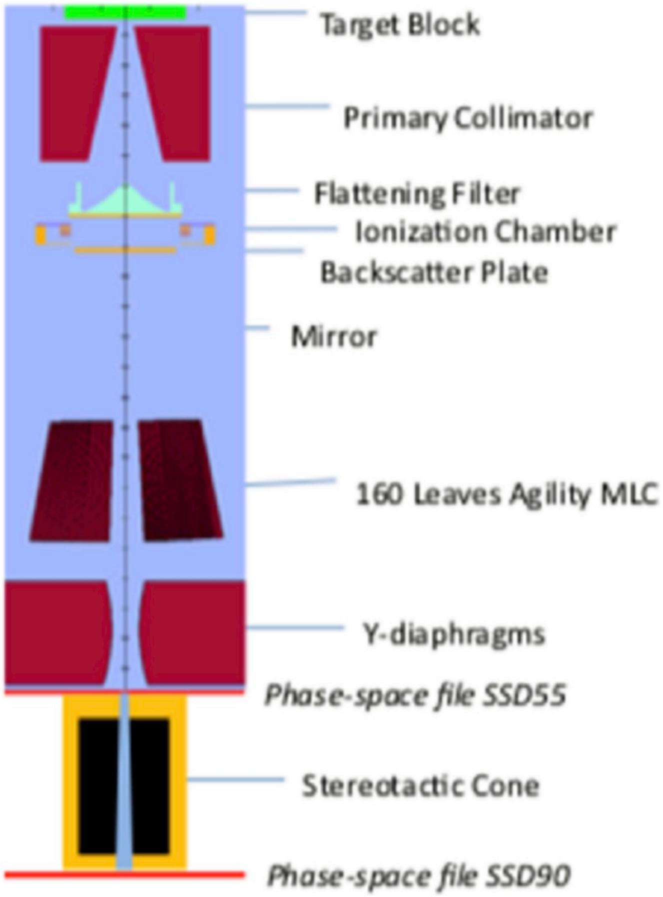

Fig. 1. Geometry of Elekta VersaHD head. Initial electron beam impact target block from the vacuum in the direction of z-axis. The component dimensions and material composition were provided by the manufacturer under nondisclosure agreement (Borzov et al., 2018).

methodology was used to minimize the uncertainties of the measurement. Therefore, the objective of this study was to measure the geometric penumbra of the circular collimator (ELEKTA Stereotactic Cone System), for ten diameters, using a mathematical tool, called gradient-based edge detection, which uses first derivative, in an edge field region, characterized by a signal profile.

2. Materials and methods

All irradiations were undertaken in the Radiotherapy Sector of the Hospital das Americas (Rio de Janeiro, Brazil) using the photon beams: 6 MV Flattening Filter and 6 MV Flattening Filter Free. To perform this study, a tertiary collimation system (ELEKTA Stereotactic Circular Collimators) was attached on a linear accelerator ELEKTA VersaHD, which also has its own collimation system: Agility Collimation system (Elekta AB, Stockholm, Sweden). The circular collimator system is adapted for treatment of stereotactic SRS indexing it in the LINAC through the base Collimator Mount (Fig. 1). The diameter of the cone collimators ranged from 5 mm to 35 mm. The aperture of the secondary collimation system Agility, used as backup for the attached system was 5 cm × 5 cm, for measurements with these circular collimators.

The EBT3 film consists of an active layer of 27 µm between two layers of opaque polyester of 120 µm, which makes it more robust. It was used in conjunction with an EPSON EXPRESSION 10000 XL film scanner (74 dpi resolution), which allows multi-channel analysis. The dose range of the EBT3 film is up to 10 Gy with the red color channel. EBT3 film is dose rate independent, close to tissue equivalent, and can be used in solid water phantoms slabs. The spatial resolution of EBT3 is mainly determined by the scanner resolution.

ImageJ is a free software, where image processing and segmentation is written in the JAVA language developed by the NIH Image, National Institutes of Health, Bethesda, USA (Ferreira and Wayne, 2012). This software allows viewing, editing, analyzing, processing, segmenting, saving and printing 8-bit, 16-bit and 32-bit images, being able to read images of different formats, among them, the TIF format (used in this study). ImageJ was developed with an open architecture that provides extensibility via plugins or macros written in the JAVA language. Therefore, with this tool the user can solve a great number of problems of image processing (Ferreira and Wayne, 2012). The representation of a pixel is the data byte type to grayscale of color images and shorts to 16-bit grayscale images. The byte and short are associated with a range of values, and it is important to note that for values of grayscale these values are positive (Ferreira and Wayne, 2012). One feature of ImageJ is the possibility of developing plugins to apply new image analysis tools as well as tools to obtain information about the image being analyzed. Plugins are classes of a programming language with the purpose of extending the functionality of a software (Oliveira et al., 2010). These plugins can be classified into two groups: those that do not require an image as input and the plugins whose input are images, the latter called Filter Plugins (Bailer, 2006). The plugins used in this study are specifically associated with image analysis, such as gradient-based edge detection. In this plugin, the first derivative is defined for a continuous function f (x) at a position x, such as a signal profile of an image. Fig. 2 shows an image and the application of a first derivative on the profile f (x) along the image center.

To perform this study, the tertiary circular collimation system (Stereotactic Circular Collimators) coupled to the Linac Elekta Versa HD was used, Fig. 1. For irradiation, the EBT3 films were placed between solid water slabs (RW3 slab phantom), Fig. 3, in a perpendicular orientation to the beam central axis (CAX), and they were irradiated by 500 monitor units (MU). The measurements were performed at 2 cm depth (isocenter plan) and 98 cm source-surface distance (SSD). According to the IAEA TRS 398 (2006), in the reference conditions (SSD = 100 cm, field = 10 cm × 10 cm and depth = 10 cm), for a linear accelerator (photon beams) with beam calibration in SSD and exposure of 1 MU is equivalent to 1 cGy at the maximum dose depth (dmax). Considering the irradiation setup for this study (SSD = 98 cm, field = 5 cm × 5 cm and depth of 2 cm), applying the correction factors, 500 MU corresponds to 501,8 cGy at 2 cm depth. For the circular fields (5 mm–35 mm in diameter), their respective output factors were applied.

Both cross-plane and in-plane beam profiles of all cone sizes were measured using EBT3 films. The exposed films were scanned by EPSON EXPRESSION 10000 XL (74 dpi resolution). Each field projection on film was considered an original image, and an inplane f(x) and cross-plane f(y) signal profiles along the midline of the image were defined. The penumbra width was defined computing the first derivative of f(x) from left to right as f'x = df(x)/dx and f(y) from gun to target (accelerator direction) as f'y = df(y)/dy and measuring the distance between points on the x-axis of signal distribution. The signal profile computing

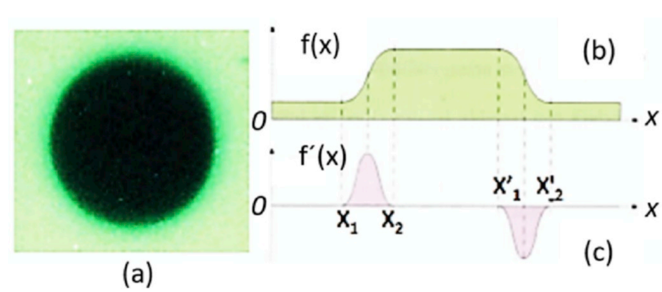

Fig. 2. a) Original image, b) Profile f (x) in the horizontal direction, c) First derivative of f(x) (Burger and Burge, 2008).

Fig. 3. Experimental arrangement for irradiation of radiochromic films with conical beams.

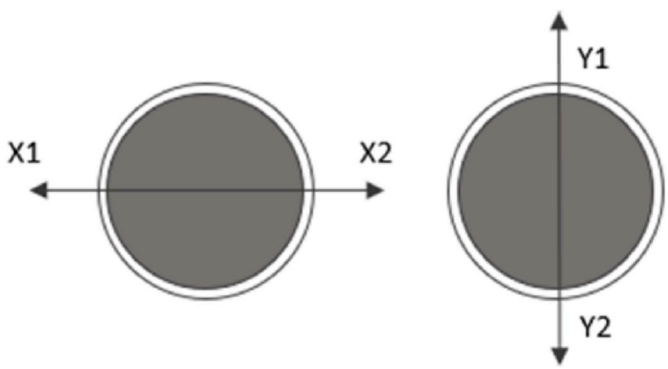

Fig. 4. Signal profile orientations.

in the central part of the beam projection from left (x1) to right (x2) and from gun (y1) to target (y2) are shown in Fig. 4. The application of this plugin is to measure the of the penumbra width, calculating the distance between the points with coordinates (x_1, 0) and (x_2, 0), (x'_1, 0) and (x'_2, 0). The values defined for x_1, x'_1, x_2 and x'_2 correspond to 20% and 80% of the signal, to characterize the penumbra region.

The original image (Fig. 5a) is uploaded to Image J and there was applied a smooth tool. A gradient edge detector plugin is used to generate vertical and horizontal derivatives and define a region between minimum and maximum signals (range of gray level), Fig. 5b. After this step, a tool is used to define a straight line to plot profile in the crossplane and inplane direction, Fig. 5 (c), (d).

3. Results and discussion

There are different methodologies for measuring the penumbra (Laub and Wong, 2003), and in this study the analysis used the ImageJ software applying an Edge Operator for Edge Detection. Films are the detectors of choice for measuring profiles, because results are obtained in a better characterization of the beam penumbra (Azcona et al., 2017). In this study, EBT3 films were used to measure the beam profiles for ELEKTA SRS cone collimators. The beam profile parameter

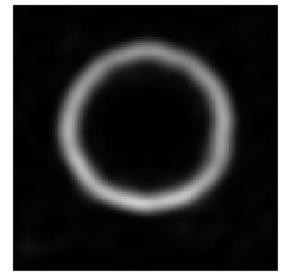

Fig. 6. Image post-processing using Edge Detection Puglin. This image corresponds to an irradiated film with cone collimator of 10 mm diameter in ImageJ software.

(penumbra width) was calculated for each cone size in the x and y profiles. Applying the first derivative using Find Edge Plugin on the film exposed the image was obtained that corresponds to the penumbra projection (Fig. 6).

To measure the penumbra width in millimeters, a calibration was made to define the factor that corrects the distance in pixels to millimeters. The measurement of the penumbra width was make using the graphics as shown at Fig. 7. The measurement was performed in the same way in the y directions. The values of penumbra width for all cones in x and y direction using 6 MV FF and 6 MV FFF beams, are presented in Table 1.

In this study an edge detection algorithm was used based on a rigorous mathematical approach. For a better understanding of this uncertainty, it is important to separate it into four parts: (a) the uncertainty of X coordinate of a point; (b) the uncertainty of Y coordinate of a point; (c) the uncertainty of determining the center of circular field; and (d) the pixel length uncertainty. Therefore, the summary defines the total uncertainty associated with the measurements of this work. The uncertainties related to the detection of edges on the x-axes and y-axes, determined by software, are estimated to be the largest possible uncertainties that the program can introduce in determining a point at the edge of the circular field (Costa, 2010). This value is estimated to be the half of a pixel length, because if the edge of the aperture is not exactly over the intersection of two pixels, but over the middle of a pixel, the program will automatically detect the border as if it were over one end of this pixel. This value is assigned a rectangular distribution because the probability of the aperture edge being contained at a given point inside a pixel is the same for all points within this pixel. For the determination of the center of the circular field in the x and y axes, the values of the edges in both axes are used, the center is determined through the average of these values. Therefore, the center of the circle is the average of a series of values. As a way of estimating a doubt for the determination of the center of the circular field, the amplitude of all possible center values used in the calculation of the mean value is determined. This procedure is valid for both axes. The pixel length in the x and y axes are values obtained from a previous calibration of the image. However, in this study, considering the pixel length, 0.34 mm, the uncertainty associated with the measurements performed in the ImageJ software corresponds to the half of the smallest unit of measurement

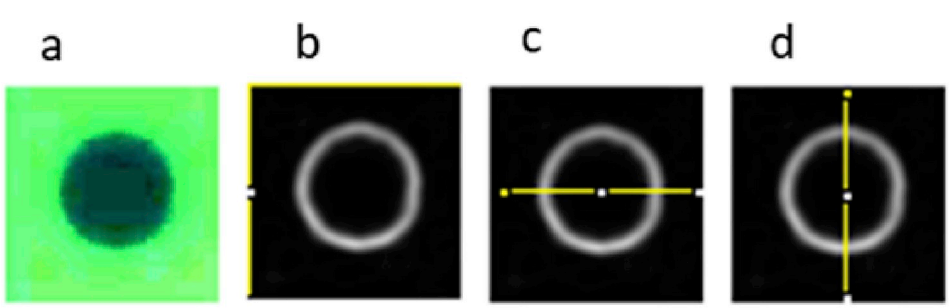

Fig. 5. Projection beam of irradiated film with cone collimator of 10 mm diameter in ImageJ software. (a) Image of film scanned and (b) Image post-processing using gradient edge detection Puglin. The yellow lines represent the straight lines to plot profiles in crossplane (c) and inplane (d). (For interpretation of the references to color in this figure legend, the reader is referred to the Web version of this article.)

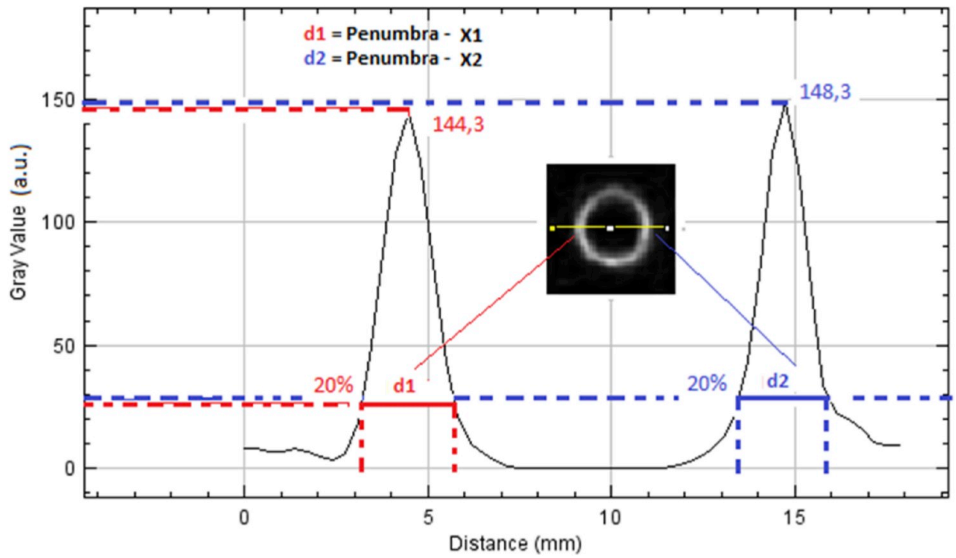

Fig. 7. Quantitative analysis of the penumbra obtained by the Edge Detection Plugin. The two peaks correspond to the first derivative, that is, the edge region of radiation field. As the dosimetric penumbra is defined in the region between 20% and 80%, the penumbra width was the distance in this part of the curve.

Table 1
Penumbra width obtained using Edge Detection Plugin (ImageJ) of films exposed to beams of Stereotactic Circular Collimator system in Elekta Versa HD.

Colimmator diameter (mm)	Penumbra Width (mm)							
	6 MV FF				6 MV FFF			
	X1	X2	Y1	Y2	X1	X2	Y1	Y2
35.0	1.8	1.8	1.8	1.8	1.8	2.0	2.0	2.0
30.0	1.8	2.0	2.3	2.0	2.0	2.0	2.0	2.3
25.0	1.8	1.8	2.0	2.0	1.8	2.0	2.0	2.0
20.0	2.0	1.8	2.0	2.0	1.7	2.0	1.8	1.8
17.5	2.0	2.0	2.3	2.4	1.8	2.0	2.0	2.0
15.0	1.5	1.5	2.2	2.0	1.7	1.8	1.8	2.0
12.5	2.0	2.3	2.3	2.3	1.7	1.8	2.3	2.3
10.0	2.0	2.0	2.0	2.3	1.7	1.8	2.3	2.0
7.5	1.8	1.8	1.7	1.6	2.0	2.3	2.0	2.0
5.0	1.6	1.8	1.8	1.8	1.8	1.8	2.0	1.8

used in this evaluation, ie ± 0.17 mm.

The mean values obtained for the 6 MV FF beams were 1.8 mm, 1.9 mm, 2.0 mm, 2.0 mm for x_1, x_2, y_1, y_2, respectively. On the other hand, the mean values of penumbra width for the 6 MV FFF beams were 1.8 mm, 2.0 mm, 2.0 mm, 2.0 mm, in the same order. This difference of x_1 and x_2 can be attributed to a subtle misalignment with respect to the central axis of beam and the conical tertiary system. For the alignment of the cone, other methodology was used, which corroborates that the methodology proposed by this work can also be used as a tool to check this parameter.

The effect of overlapping penumbra on the FWHM of the lateral beam profile for small fields illustrates the apparent field widening compared to the collimator settings (IAEA, 2017). In addition to the longer forward electron range, higher energy beams have also a longer lateral electron range that increases the penumbra width significantly. Even for conventional broad fields, when tertiary collimation is used for reduction of their penumbra, the effect of the detector's finite volume can lead to inaccuracies in the determination of the penumbra width. For these reasons, in this study the detector used was a EBT3 film. This film (EBT3) has sufficient spatial resolution for small field dosimetry. It was observed that penumbra width measured in x and y directions for cones is less than linac equivalent square fields (Costa, 2010). Smaller penumbra for cones in comparison with penumbra for equivalent square field is partially due to cones closer to the phantom surface and different geometry and scattering in cones in comparison with jaws (Borzov et al., 2018). Therefore, in this study, the proposed methodology was applied to 6 MV: FF and FFF beams, and the results obtained for the penumbra width presented a small difference. The biggest difference between 6 MV FF and FFF was 0.5 mm. Considering the penumbra width found by Al Shukaili et al. (2017) and Yarahmadi et al. (2013), this methodology underestimates the values of penumbra width. In general, the penumbra width values were close to those obtained during commissioning. Borzov et al. (2018) obtained a value of 2 mm for the cone (10 mm diameter) using the same Cone System. However, a specific point for this analysis is the plane where data were taken, because the distance from the source is smaller than that used in literature. Therefore, it is considered important to apply this methodology to other setups.

4. Conclusion

The values show that a quantitative analysis of the penumbra width of small fields is possible using the mathematical toll Gradient-Based Edge Detection. This tool can be used in some softwares as Find Edge Plugin. The results obtained in this study corroborate the expected values of penumbra for the Elekta Stereotactic Cone Collimation System, as well as suggested, through other studies, a potential tool to evaluate the alignment of this tertiary system. The methodology used allows to affirm that the use of an edge detection operator as a tool for the evaluation of penumbra width is possible. However, some of the results suggest that the application of image evaluation features, such as smoothing, can help in the evaluation of signal profiles for penumbra calculation.

Acknowledgments

The authors acknowledge the partial financial support from the Brazilian agencies: CNEN, CNPq (Project 301335/2016-8) and CAPES (Project 554/2018).

References

AAPM (American Association of Physicists in Medicine), 1999. TG-51: protocol for clinical reference dosimetry of high-energy photon and electron beams. Med. Phys. 26 (9), 1847–1870.

Al Shukaili, K., Petasecca, M., Newall, M., Espinoza, A., Perevertaylo, V.L., Corde, S., Lerch, M., Rosenfeld, A.B., 2017. A 2D silicon detector array for quality assurance in

small field dosimetry: DUO. Med. Phys. 44, 628–636.
Azcona, J.D., Barbés, B., Morán, V., Burguete, J., 2017. Commissioning of small field size radiosurgery cones in a 6-MV flattening filter-free beam. Med. Dosim. 42 (4), 282–288.
Bailer, W., 2006. Writing ImageJ Plugins—A Tutorial 1.71 Hagenberg, Austria.
Borzov, E., Nevelsky, A., Bar-Deroma, R., Orion, I., 2018. Dosimetric characterization of Elekta stereotactic cones. J. Appl. Clin. Med. Phys. 19 (1), 194–203.
Burger, W., Burge, M.J., 2008. Digital Imaging Processing: an Algorithmic Introduction Using Java, first ed. Springer, New York.
Costa, P.B., 2010. Determination of measurement uncertainties in the calibration of the area of circular apertures. Produto Produção. 11, 70–79 (In Portuguese).
Ferreira, T., Wayne, R., 2012. ImageJ User Guide – IJ 1.46r. ImageJ FIGI.
IAEA (International Atomic Energy Agency), 2006. Absorbed Dose Determination in External Beam Radiotherapy: an International Code of Practice for Dosimetry Based on Standards of Absorbed Dose to Water, Technical Report Series, No. 398. Vienna.
IAEA (International Atomic Energy Agency), 2017. Dosimetry of Small Static Fields Used in External Beam Radiotherapy: an International Code of Practice for Reference Dose and Relative Dose Determination, Technical Report Series, No. 483. Vienna.
Laub, W.U., Wong, T., 2003. The volume effect of detectors in the dosimetry of small fields used in IMRT. Med. Phys. 30, 341–347.
Oliveira, R.S.M.F., Oliveira, F.A.M., Pinheiro, H.S., 2010. Programming the ImageJ software for an automatic selection of areas marked by immunohistochemistry and stained with DAB chromogen and counterstained by hematoxylin. Rev. Int. Est. Exp. 3, 76–80 (In Portuguese).
Schell, M., Bova, F.J., Larson, D.A., Leavitt, D.D., Latz, W.R., Podgorsak, E.B., Wu, A., 1995. Stereotactic Radiosurgery. AAPM Report No. 54. Report of Task Group 42 Radiation Therapy Committee. American Institute of Physics, New York.
Yarahmadi, M., Allahverdi, M., Nedaie, H.A., Asnaashari, K., Vaezzadeh, S.A., Sauer, O.A., 2013. Improvement of penumbra for small radiosurgical fields using flattening filter free low megavoltage beams. Z. Med. Phys. 23, 291–299.